Variational bounds for lattice fermion models II. Extended Hubbard model in the atomic limit

1993 J. Phys. A: Math. Gen. 26 4497

(http://iopscience.iop.org/0305-4470/26/18/017)

J. Phys. A: Math. Gen. 26 (1993) 4497–4511. Printed in the UK

Variational bounds for lattice fermion models II: extended Hubbard model in the atomic limit

R J Bursill and C J Thompson

Mathematics Department, University of Melbourne, Parkville, Victoria 3052, Australia

Received 12 March 1993

Abstract. In this paper we derive a mean-field expression for the Helmholtz free energy of the extended Hubbard model with on-site repulsion and longer range attraction in the atomic limit. The mean-field free energy is exact in the infinite-dimensional and long-range limits and reduces to the exact ground state energy at $T=0$. Implications for the phase diagram of the extended Hubbard model are discussed.

1. Introduction

The extended Hubbard model has been the subject of intense study [1–3] as a model for high-temperature superconductivity. The Hamiltonian is given by

$$\mathcal{H}_{\mathrm{EHM}}=\sum_{k\sigma}\varepsilon_k c^{\dagger}_{k\sigma}c_{k\sigma}+U\sum_i n_{i\uparrow}n_{i\downarrow}-\sum_{i\neq j}J_{ij}n_i n_j \tag{1.1}$$

where $c^{\dagger}_{k\sigma}$ ($c_{k\sigma}$) is the creation (annihilation) operator for particles with wavevector k, kinetic energy ε_k and spin $\sigma=\uparrow$ or $\downarrow$, $n_{i\sigma}$ is the number operator for particles on site i with spin σ, $n_i=n_{i\downarrow}+n_{i\uparrow}$, U is the on-site interaction strength and J_{ij} measures the strength of the longer-range interaction.

In [1–3] the thermodynamic phases of the extended Hubbard model are studied by comparing various mean-field approximations. The validity of these approximation schemes has not, however, been thoroughly investigated for lattice fermion models such as (1.1).

For instance, it would be of great interest to establish a comprehensive mean-field theory for these systems which is exact in the infinite-dimensional limit and/or the long-range limit of Kac potentials where it is known that lattice spin models approach their well known mean-field theories [4]. Limited exact results have been obtained by Vollhardt [5] and others [6] in high spatial dimension but as shown in a recent paper [7] even in the simple case of spinless fermions with an attractive nearest-neighbour interaction there can be no simple mean-field theory which is exact in the infinite-dimensional limit.

We leave the question of the validity of mean-field theories for the extended

0305-4470/93/184497+15 $07.50

Hubbard model (1.1) to future publications. In this paper we concentrate on the atomic limit ($\varepsilon_k \equiv 0$) of (1.1), i.e.

$$\mathcal{H} = U \sum_i n_{i\uparrow} n_{i\downarrow} - \sum_{i \neq j} J_{ij} n_i n_j. \tag{1.2}$$

We derive a mean-field expression for the Helmholtz free energy of (1.2) and show (in the appendix) that this expression is exact in the infinite-dimensional limit and the long-range limit of Kac potentials. Also in the $T=0$ limit the mean-field free energy reduces to exact ground-state energy.

We note that (1.2) is simply the Hamiltonian of a classical, two-component lattice gas. We consider the case where $U>0$ and

$$J_{ij} = \tilde{J}(\|i-j\|) \tag{1.3}$$

where $\tilde{J}(x)$ is a positive, monotone decreasing function. That is, the on-site term is repulsive and the longer-range term is attractive. We also scale units so that

$$\sum_j J_{ij} = 1. \tag{1.4}$$

Finally we note that in the hard-core limit ($U \to \infty$) (1.1) has been put forward as a lattice-gas model of liquid He^3 [8].

In the following section we derive the mean-field expression for the Helmholtz free energy of (1.2). The critical temperature is derived and the ordered state (below criticality) is characterized and interpreted. In section 3 these results are discussed in the context of the extended Hubbard model.

2. Mean-field theory

2.1. Helmholtz free energy and the variational principle

We consider (1.2) on a d-dimensional hypercubic lattice with volume $V = L^d$. The grand canonical partition function is given by

$$\mathfrak{Q} = \mathrm{Tr}\, e^{-\beta(\mathcal{H} - \mu \mathcal{N})} \tag{2.1}$$

where $\beta = 1/kT$ with k Boltzmann's constant and T the absolute temperature, μ is the chemical potential and $\mathcal{N}$ is the number operator.

The thermodynamic potential is defined by

$$\chi = V^{-1} \log \mathfrak{Q} \tag{2.2}$$

where the equation

$$n = \lim_{V \to \infty} \frac{\langle \mathcal{N} \rangle}{V} \tag{2.3}$$

provides a relationship between the (average) particle density n and the chemical potential where $\langle\rangle$ denotes the thermodynamic average defined by

$$\langle \mathcal{A} \rangle = \mathcal{Q}^{-1} \operatorname{Tr} \mathcal{A} e^{-\beta \mathcal{H}}. \tag{2.4}$$

With μ and χ considered as functions of n and T the Helmholtz free energy is given by

$$\psi = \lim_{V \to \infty} (\mu - \chi / n\beta). \tag{2.5}$$

A variational upper bound can be generally obtained by writing $\mathcal{H}$ in the form

$$\mathcal{H} = \mathcal{H}_0 + \mathcal{H}_1 \tag{2.6}$$

with $\mathcal{H}_0$, the reference Hamiltonian, chosen so that the reference grand canonical partition function

$$\mathcal{Q}_0 = \operatorname{Tr} e^{-\beta(\mathcal{H}_0 - \mu N)} \tag{2.7}$$

can be calculated easily but is also representative of the basic physics of the system.

With $\mathcal{Q}$ replaced by $\mathcal{Q}_0$ in (2.1) one obtains the reference thermodynamic potential χ_0 and the corresponding reference free energy

$$\psi_0 = \lim_{V \to \infty} (\mu - \chi_0 / n\beta) \tag{2.8}$$

where in the equation (2.3) for n, the thermodynamic average is taken with respect to the reference system, i.e. $\mathcal{Q}$ and $\mathcal{H}$ in (2.4) replaced, respectively, by $\mathcal{Q}_0$ and $\mathcal{H}_0$.

It follows from Jensen's inequality that

$$\psi \leq \psi_0 + \lim_{V \to \infty} \langle \mathcal{H}_1 \rangle_0 / nV \equiv \psi_{\mathrm{mf}} \tag{2.9}$$

where $\langle \mathcal{H}_1 \rangle_0$ denotes the average of $\mathcal{H}_1$ with respect to the reference system.

2.2. *Reference Hamiltonian and the mean-field free energy*

We make the choice

$$\mathcal{H}_0 = U \sum_i n_{i\uparrow} n_{i\downarrow} \tag{2.10}$$

so from (1.2) and (2.6) we have

$$\mathcal{H}_1 = -\sum_{i \neq j} J_{ij} n_i n_j. \tag{2.11}$$

With this choice of $\mathcal{H}_0$, ψ_{mf} and μ are easily calculated:

$$\psi_{\mathrm{mf}} = \psi_0 - n \tag{2.12}$$

$$\chi_0 = \log(1 + 2z + z^2 e^{-\beta U}) \tag{2.13}$$

with ψ_0 determined by (2.8) and $z = e^{\beta\mu}$ given by

$$z = \frac{e^{\beta U}}{2 - n} [n - 1 + \{(n-1)^2 + n(2-n) e^{-\beta U}\}^{1/2}]. \tag{2.14}$$

The upper bound (2.9) can, however, be improved by noting that the exact free energy ψ, considered as a function of the specific volume $v \equiv 1/n$, must be C^1, monotone decreasing and concave [9]. ψ_{mf} is C^1 but need not be monotone decreasing or concave. We thus define the (superior) upper bound

$$\psi \leqslant CE\{\psi_{mf}\} \equiv \psi vw \tag{2.15}$$

where CE denotes the concave envelope. That is, as a function of v, ψvw is the greatest, C^1, monotone decreasing, concave function which is bounded above ψ_{mf}. In the appendix we show that equality between ψ_{vw} and ψ is actually achieved in the infinite dimensional and Kac limits.

We denote the concave envelope by ψvw because in the $U=0$ case ψvw reduces to the lattice gas version of the Van der Waals–Maxwell free energy [9]. In the sequel we shall say that ψ_{mf} is stable if it is monotone decreasing and concave in v. In such cases $\psi_{vw} \equiv \psi_{mf}$ for all v.

2.3. *Critical temperature*

To determine where ψ_{mf} is stable we calculate its derivatives with respect to v. The mean-field pressure is defined by

$$p_{mf} \equiv -\frac{\partial \psi_{mf}}{\partial v} \tag{2.16}$$

A routine calculation yields

$$p_{mf} = p_0 - n^2 \tag{2.17}$$

where

$$p_0 \equiv -\frac{\partial \psi_0}{\partial v} = \chi_0/\beta. \tag{2.18}$$

Clearly ψ_{mf} is stable if and only if p_{mf} is positive and monotone decreasing in v. It is easily established that p_{mf} is positive and monotone decreasing if v is sufficiently small or large. It follows that ψ_{mf} is stable if and only if p_{mf} has no turning points. Differentiating (2.17) we find that the condition for p_{mf} to have turning points is

$$\frac{\partial \mu}{\partial n} = 2 \tag{2.19}$$

or, alternatively

$$U = F(n, \beta U) \tag{2.20}$$

where

$$F(n,x) = 2x\left[\frac{1}{2-n} + \frac{1+(1-n)(e^{-x}-1)/\{(n-1)^2+n(2-n)\,e^{-x}\}^{1/2}}{n-1+\{(n-1)^2+n(2-n)\,e^{-x}\}^{1/2}}\right]^{-1}, \tag{2.21}$$

Plots of F versus n for various values of x are given in figure 1. $F(2-n,x) = F(n,x)$ so turning points of p_{mf} occur in pairs equally spaced about $n=1$. F is monotone increasing in n on $[0,1]$ for $0 \leqslant x \leqslant 2\log 2$. For $x > 2\log 2$ F is not monotone on $[0,1]$

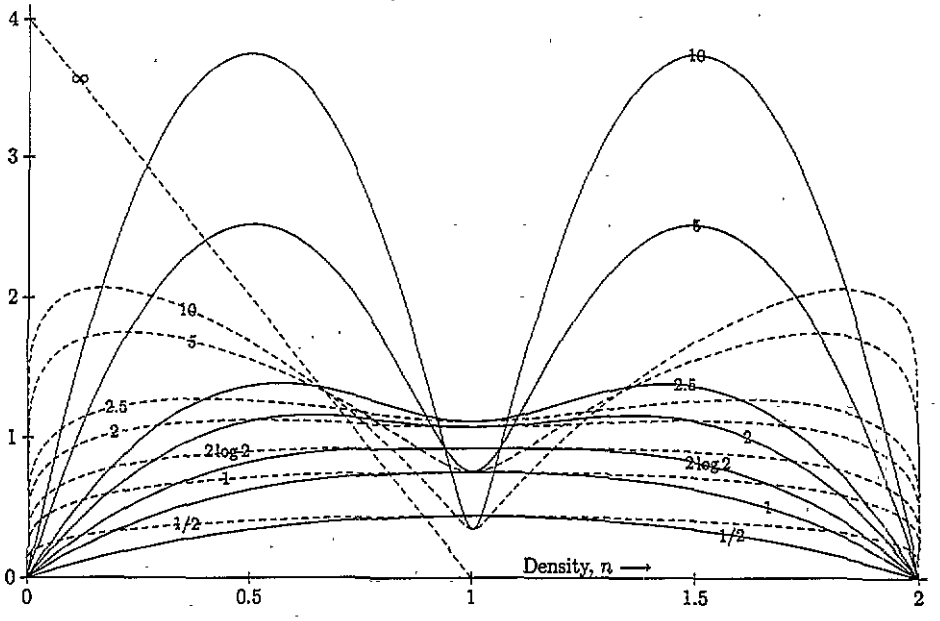

Figure 1. $F(n,x)$ and $G(n,x)$ (dashed) versus n for various values of x.

but takes on a maximum at a density which we denote by $n^*(x)$ ($\partial^2 F/\partial n^2(1,x) = 2x(e^{x/2}-2)$ vanishes when $x = 2\log 2$.).

We make the definition

$$F_{\max}(x) \equiv \max_{0\leqslant n\leqslant 1} F(n,x)$$
$$= \begin{cases} F(1,x) & 0 \leqslant x \leqslant 2\log 2 \\ F(n^*(x),x) & x > 2\log 2. \end{cases} \tag{2.22}$$

$F_{\max}(x)$ is monotone increasing in x. It follows that there is a well defined critical temperature T_c above which p_{mf} has no turning points (and hence ψ_{mf} is stable) defined by

$$U = F_{\max}(U/T_c). \tag{2.23}$$

For $T < T_c$, p_{mf} may have two or four turning points or, equivalently, ψ_{mf} may have two or four inflexion points. We note that $T_c = \frac{2}{3}$ at $U = 4\log 2/3$ ($F(1, 2\log 2) = 4\log 2/3$). Using (2.22) then we see that (2.23) reduces to

$$U = F(1, U/T_c) \tag{2.24}$$

for $0 \leqslant U \leqslant 4\log 2/3$ and

$$U = F(n^*(U/T_c), U/T_c) \tag{2.25}$$

for $U > 4\log 2/3$. T_c is graphed as a function of U in figure 2. We may define a critical density n_c by

$$n_c = \begin{cases} 1 & 0 \leqslant U \leqslant 4\log 2/3 \\ n^*(U/T_c) & U > 4\log 2/3 \end{cases} \tag{2.26}$$

2.4. The nature of the concave envelope and the order parameter below criticality

In the case where ψ_{mf} has two points of inflexion, ψ_{vw} is obtained from a double tangent construction as shown in figure 3.

$$\psi_{vw} = \begin{cases} \psi_{mf} & \text{for } v \leqslant v_l \\ \psi_l + \dfrac{\psi_g - \psi_l}{v_g - v_l}(v - v_l) & \text{for } v_l < v < v_g \\ \psi_{mf} & \text{for } v \geqslant v_g \end{cases} \tag{2.27}$$

where $\psi_l = \psi_{mf}(v_l)$ and $\psi_g = \psi_{mf}(v_g)$ with v_l and v_g interpreted as the liquid and gas specific volumes, respectively. The region $v_l < v < v_g$ in which $\psi_{vw} < \psi_{mf}$ is interpreted as the *coexistence* region.

If ψ_{mf} has four points of inflexion then ψ_{vw} may be given by the *simple* double tangent construction (2.27) as shown in figure 4. On the other hand, a pair of double tangent constructions may be required as shown in figure 5, namely

$$\psi_{vw} = \begin{cases} \psi_{mf} & 1/2 \leqslant v \leqslant v_4 \\ \psi_4 + \dfrac{\psi_3 - \psi_4}{v_3 - v_4}(v - v_4) & v_4 < v < v_3 \\ \psi_{mf} & v_3 \leqslant v \leqslant v_2 \\ \psi_2 + \dfrac{\psi_1 - \psi_2}{v_1 - v_2}(v - v_2) & v_2 < v < v_1 \\ \psi_{mf} & v \geqslant v_1. \end{cases} \tag{2.28}$$

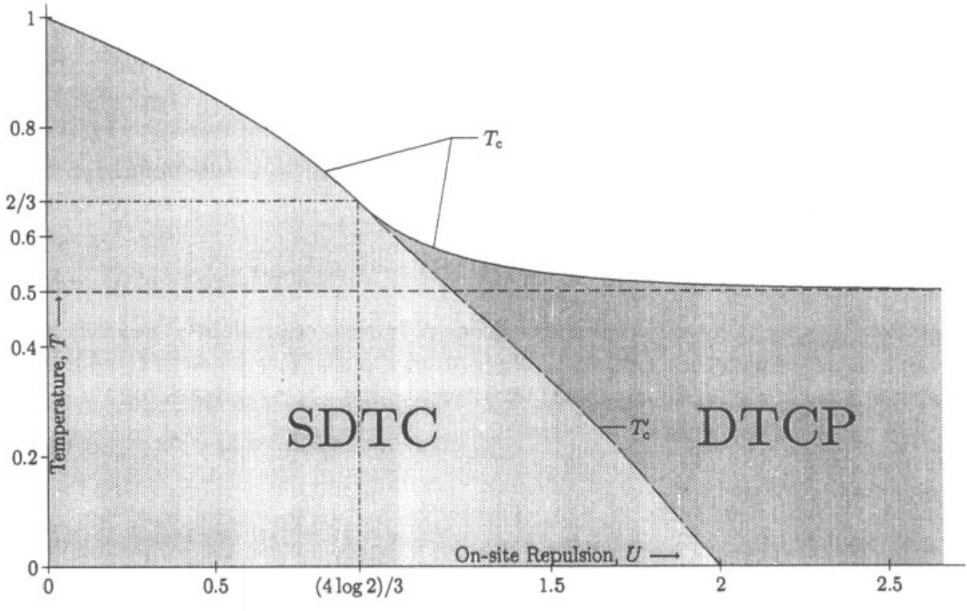

Figure 2. Phase diagram for the extended Hubbard model with on-site repulsion and longer-range attraction in the atomic limit including T_c and T_c' as functions of U. Shading indicates whether the concave envelope is a simple double tangent construction (light) or a double tangent construction pair (dark).

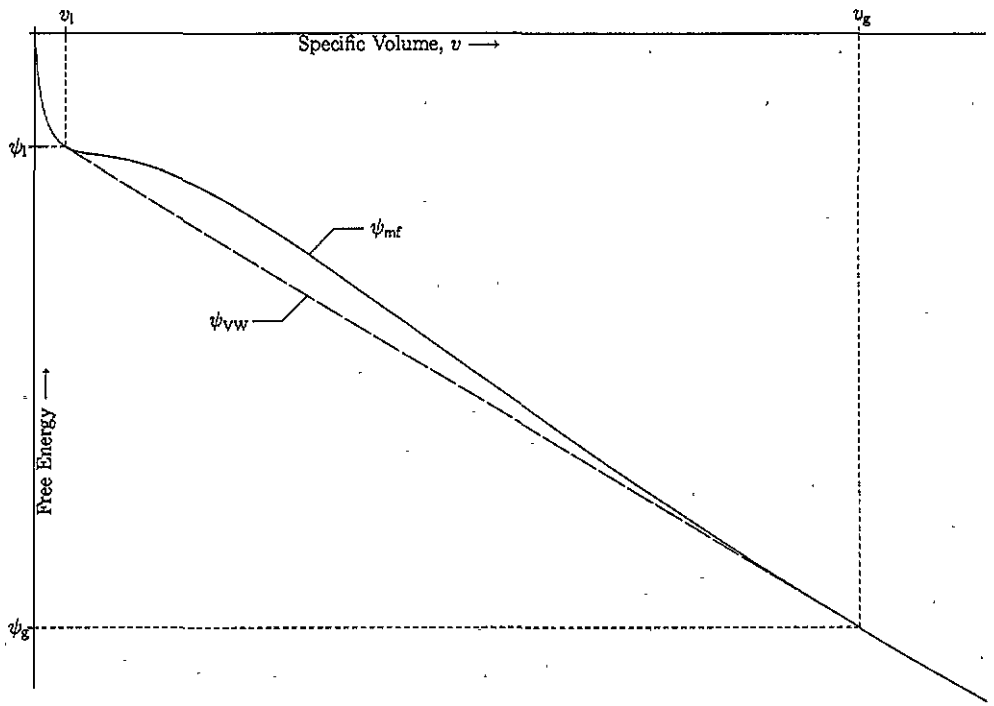

Figure 3. Double tangent construction for the mean-field free energy ψ_{mf} in a case where ψ_{mf} has two points of inflexion.

The coexistence regions in this case are $v_4 < v < v_3$ and $v_2 < v < v_1$.

When ψ_{vw} is given by (2.27) it can be shown by symmetry or by direct calculation that

$$n_l = 2 - n_g \tag{2.29}$$

where $n_l \equiv 1/v_l$ and $n_g \equiv 1/v_g$. The equation determining n_g is found to be

$$U = G(n_g, \beta U) \tag{2.30}$$

where

$$G(n,x) \equiv 2x(n-1)\left[\tanh^{-1}(n-1) + \tanh^{-1}\frac{n-1}{\{(n-1)^2 + n(2-n)\,e^{-x}\}^{1/2}}\right]^{-1}. \tag{2.31}$$

Plots of G versus n for various values of x are included in figure 1. Note that when ψ_{mf} has four points of inflexion there is a spurious solution of (2.30) that corresponds to the *convex* envelope. A plot of the convex envelope is included in figure 4.

We note that in the limit $U \to 0$ (2.30) reduces to the well known Van der Waals equation for a lattice gas, namely

$$n_g - 1 = \tanh \beta (n_g - 1). \tag{2.32}$$

When ψ_{vw} is given by (2.28) we again have symmetries

$$n_4 = 2 - n_1 \tag{2.33}$$

$$n_3 = 2 - n_2 \tag{2.34}$$

where $n_i \equiv 1/v_i$. The equations determining n_1 and n_2 do not simplify to forms like (2.29) and (2.30) except in the limit $U \to \infty$ where we have

$$n_2 = 1 - n_1 \tag{2.35}$$

and

$$2(n_1 - 1/2) = \tanh \beta (n_1 - 1/2). \tag{2.36}$$

It remains to determine which of the two forms, (2.27) or (2.28) gives the concave envelope when ψ_{mf} has four points of inflexion. It is found that when both constructions are possible (2.27) gives the concave envelope if

$$\psi_1 + \frac{\psi_g - \psi_l}{v_g - v_l}(1 - v_l) \leqslant \psi_{mf}(n = 1) \tag{2.37}$$

and (2.28) gives the concave envelope otherwise. We now characterize the form of the concave envelope below criticality. There are three regions of interest for U.

1 $0 \leqslant U \leqslant 4 \log 2/3$
For $0 \leqslant T < T_c$ ψ_{vw} is given by (2.27) even for low temperatures where ψ_{mf} has four inflexions.

2 $4 \log 2/3 < U < 2$
For T just below T_c, ψ_{vw} is given by (2.28), the simple construction (2.27) not being possible because (2.30) possesses no solutions. As T is decreased (2.30) develops solutions and both constructions, (2.27) and (2.28) are possible. As T passes

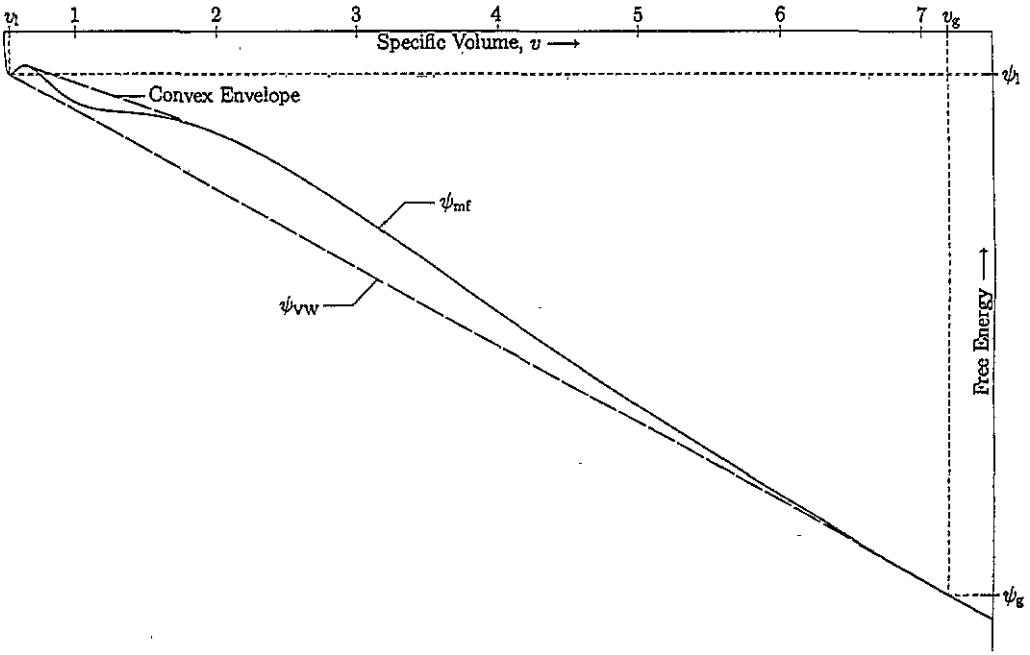

Figure 4. Simple double tangent construction for the mean-field free energy ψ_{mf} in a case where ψ_{mf} has four points of inflexion. A *convex* envelope construction is also shown and corresponds to a spurious solution of the equation determining the gas and liquid specific volumes.

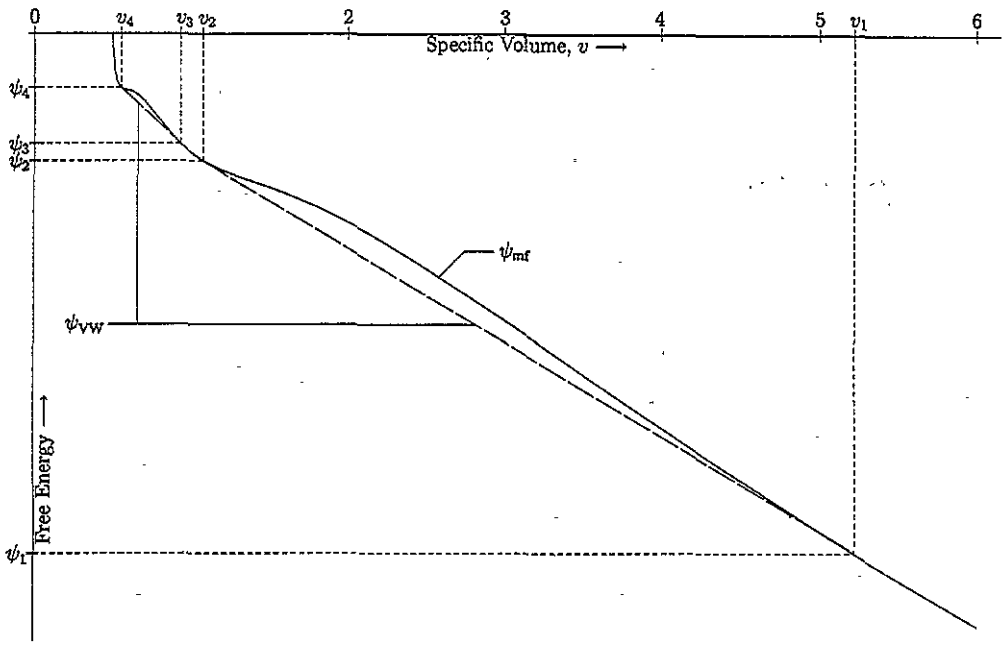

Figure 5. Pair of double tangent constructions for the mean-field free energy ψ_{mf} in a case where ψ_{mf} has four inflexions.

through a critical value T_c' the two constructions coalesce ie v_2, $v_3 \to 1^{+,-}$, $v_1 \to v_g^+$ and $v_4 \to v_l^-$ as $T \to (T_c')^+$. For $T_c' < T < T_c$, ψ_{vw} is given by (2.28). For $0 \leqslant T < T_c'$, ψ_{vw} is given by (2.27), (2.28) not being possible. From (2.37) we see that the condition determining T_c' is

$$\psi_l + \frac{\psi_g - \psi_l}{v_g - v_l}(1 - v_l) = \psi_{mf}(n=1) \qquad \text{at } T = T_c' \tag{2.38}$$

A plot of T_c' versus U is included in figure 2.

3 $U \geqslant 2$

For $0 \leqslant T < T_c$, ψ_{vw} is given by (2.28) even though the simple construction is possible ((2.30) has solutions) for low enough temperatures—at least for $2 \leqslant U < 4$ (figure 1).

In figure 2 we indicate by shading which of the two constructions, (2.27) (the simple double tangent construction) or (2.28) (the double tangent construction pair) gives the concave envelope. The coexistence region in the (n, T) plane is sketched in figure 6 for each of the regions of interest for U.

Finally note that there is a well defined order parameter, $v_g - v_l$ for $0 \leqslant U \leqslant 4 \log 2/3$ and $v_3 - v_4$ for $U > 4 \log 2/3$, which vanishes as $T \to T_c^-$.

2.5. *Ground state energy estimates and physical interpretation of the condensed phases*

In order to determine the estimate of the ground state energy (the $T = 0$ limit of ψ_{vw}) we begin by indicating why the ψ_{vw} at $T = 0$ is given by (2.27) for $0 \leqslant U \leqslant 2$ and by (2.28) for $U > 2$.

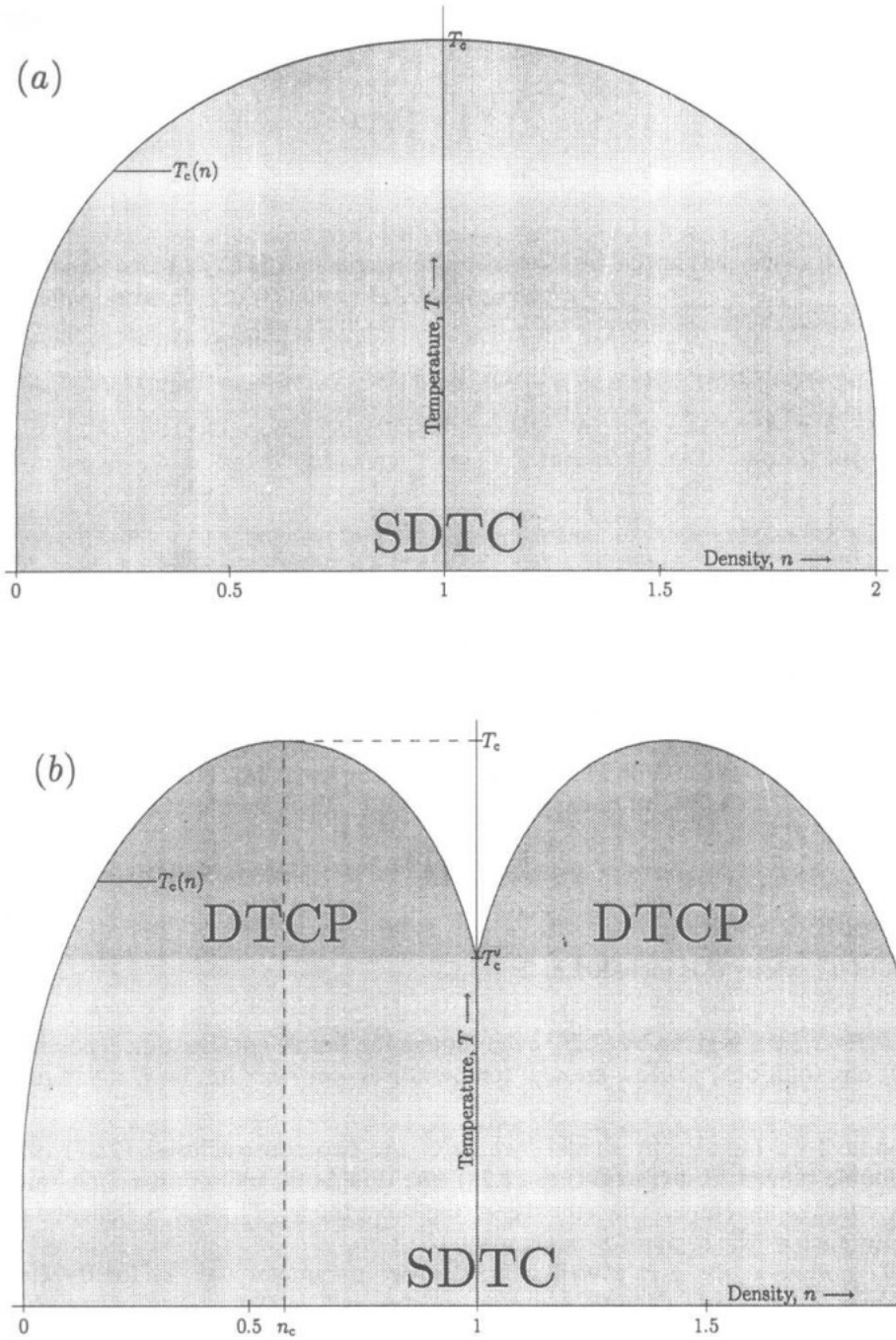

Figure 6. The coexistence region (shaded) in the (n, T) plane for the three regions of interest: (a) $0 \leq U \leq 4 \log 2/3$, (b) $4 \log 2/3 < U < 2$; and (c) $U \geq 2$. In the light shaded regions the concave envelope is a simple double tangent construction (SDTC) and in the dark shaded regions the concave envelope is a double tangent construction pair (DTCP). $T_c(n)$, the density-driven critical temperature is the temperature which bounds the coexistence region.

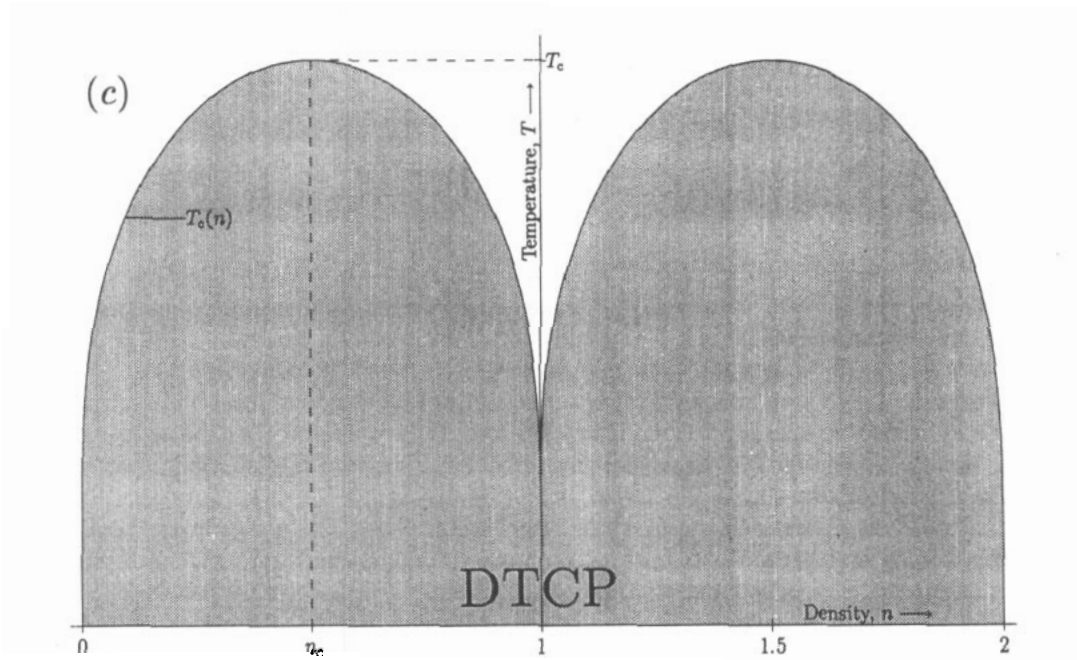

Figure 6c.

We note from figure 1 that (2.30) has solutions (the simple double tangent construction (2.27) is possible) for sufficiently small T as long as $0 \leqslant U < 4$. From (2.30) it can be shown that

$$n_g \sim \begin{cases} e^{-2(1-U/4)\beta} & 0 \leqslant U < 2 \\ e^{-\beta} & 2 \leqslant U < 4 \end{cases} \tag{2.39}$$

as $T \to 0$. Using (2.8), (2.12), (2.13), (2.14) and (2.39) we find that

$$\psi_g \sim -2(1-U/4) + O(1/\beta) \tag{2.40}$$

$$\psi_1 \sim \begin{cases} -2(1-U/4) + O(e^{-2(1-U/4)\beta}) & 0 \leqslant U < 2 \\ -2(1-U/4) + O(e^{-\beta}) & 2 \leqslant U < 4 \end{cases} \tag{2.41}$$

as $T \to 0$. It follows from (2.27), (2.29), (2.39), (2.40) and (2.41) that the $T=0$ limit of (2.27) is identically $-2(1-U/4)$ for $0 \leqslant U < 4$.

On the other hand it is easily derived from (2.8), (2.12), (2.13) and (2.14) that

$$\lim_{T \to 0} \psi_{mf} = \begin{cases} -n & 0 \leqslant n \leqslant 1 \\ U(1-1/n) - n & 1 < n \leqslant 2 \end{cases} \tag{2.42}$$

so the limiting form of (2.27) only lies below

$$\lim_{T \to 0} \psi_{mf}(n=1) = -1$$

if $0 \leqslant U \leqslant 2$. From (2.37) then, the ground state energy estimate is given by the $T=0$ limit of (2.28) for $U > 2$. It can be shown in such cases that v_3, $v_2 \to 1$, $v_4 \to \frac{1}{2}$ and $v_1 \to \infty$ as $T \to 0$.

Combining the above results and using (2.28) and (2.42) we arrive at the ground-state energy estimate

$$\lim_{T\to 0} \psi_{vw} = \begin{cases} -2(1-U/4) & 0 \leqslant n \leqslant 2 \qquad\qquad 0 \leqslant U \leqslant 2 \\ \begin{cases} -1 & 0 \leqslant n \leqslant 1 \\ -2(1-U/4)+(1-U/2)(1/n-1/2) & 1 < n \leqslant 2 \end{cases} & \qquad\qquad U > 2. \end{cases} \tag{2.43}$$

Now the exact N-particle ground state has zero magnetization ($N/2$ up particles and $N/2$ down particles) if $0 \leqslant U \leqslant 2$, the N particles forming a tightly packed cluster of $N/2$ doubly occupied sites.

If $U > 2$ and $N \leqslant V$ then the ground state is again a tightly packed cluster but of N singly occupied sites with no specific magnetization. If $N > V$ then at least $N - V$ of the sites must be double occupied. The ground state consists of a tightly packed cluster of $N - V$ double occupied sites, the rest of the sites being singly occupied again with no specific magnetization.

It is easily established using (1.2) that the ground state energy estimate (2.43) equates to the exact ground state energy. We note that the ground state is a condensed state in that particles form a macroscopic cluster. For $0 \leqslant U \leqslant 2$, the cluster is as tightly bound as possible—all occupied sites are doubly occupied. For $U > 2$ however, double occupancies are energetically unfavourable, and the cluster is less tightly bound, taking up a greater volume. Clusters form as a result of the interaction being predominantly attractive. The on-site repulsion, if sufficiently strong, frustrates this process.

From the exact ground state, we are naturally lead to an interpretation of the subcritical phases depicted in figure 2 and figure 6. Both are condensed states in that cluster formation occurs. The clusters are more tightly bound (consisting mainly of doubly occupied sites), however, when the concave envelope is a SDTC and less tightly bound (with double occupancies less favoured) when the concave envelope is a DTCP.

3. Summary and discussion

In this paper we have derived a mean-field expression for the Helmoltz free energy of the extended Hubbard model with on-site repulsion and longer-range attraction in the atomic limit. The mean-field theory is valid in the sense that it recovers the exact Helmholtz free energy in the $d = \infty$ and Kac limits as well as the exact ground-state energy.

The relevance of this study is that the phase diagram (figure 2) the coexistence regions (figure 6) and the interpretation of the phases described in section 2.5 should apply to the extended Hubbard model when the couplings are strong compared with the kinetic energy.

We may define the *density-driven critical temperature* $T_c(n)$ as the temperature, for a given value of n, at which ψ_{vw} is non-analytic. The coexistence region is the region in the (n, T) plane which lies below $T_c(n)$. We see from figure 6 that for $U > (4 \log 2/3)$ $T_c(n)$ exhibits non-monotonicity in n on $[0, 1]$, half filling ($n = 1$) being a local minimum as opposed to a global maximum for $T_c(n)$. For $U > 2$ the half-filled ground state is actually non-ordered and the non-monotonicity of $T_c(n)$ is qualitatively similar to that observed in the mean-field studies of the extended Hubbard model [1–3] in the case where a spin-triplet pairing ansatz is employed in deriving a density-driven

critical temperature. Such non-monotonicity is qualitatively similar to the *inverse parabolic* behaviour observed in the hole dependence of superconducting critical temperature of the cuprate superconductors [10].

In future studies we will consider the question of the validity of mean-field theories for the extended Hubbard model where various pair correlations like those studied in [1] must be incorporated into the reference Hamiltonian.

Acknowledgments

R J Bursill gratefully acknowledges the support of an Australian Postgraduate Research Award.

Appendix. Exactness of the mean-field theory in the $d=\infty$ limit and the long-range limit of Kac potentials

To show that ψ_{vw} equates to ψ in the $d=\infty$ and Kac limits we first derive an equivalent mean-field lower bound for the grand canonical potential. Writing

$$\mathcal{H}_1 = -\sum_{i\neq j} J_{ij}(n_i-\rho)(n_j-\rho) \tag{A.1}$$

we have (using (1.2), (1.4), (2.6) and (A.1))

$$\mathcal{H}_0 = 2\rho\mathcal{N} + V\rho^2 + U\sum_i n_{i\uparrow}n_{i\downarrow}. \tag{A.2}$$

Applying Jensen's inequality we obtain

$$\mathcal{Q} \geq \mathcal{Q}_0 \exp[-\beta\langle\mathcal{H}_1\rangle_0] \tag{A.3}$$

where $\mathcal{Q}_0$ is defined by (2.7). Using (2.1), (2.2), (2.7) and (A.3) we then have

$$\chi \geq \chi_0 - \beta V^{-1}\langle\mathcal{H}_1\rangle_0 \equiv \chi_{mf}. \tag{A.4}$$

A simple calculation yields

$$\chi_{mf} = \log(1+2z e^{2\beta\rho} + z^2 e^{4\beta\rho} e^{-\beta U}) - \beta\rho^2 + \beta(\bar{n}-\rho)^2 \tag{A.5}$$

where

$$\bar{n} \equiv \langle n_i\rangle_0 = \frac{2z e^{2\beta\rho}(1+z e^{2\beta\rho} e^{-\beta U})}{1+2z e^{2\beta\rho} + z^2 e^{4\beta\rho} e^{-\beta U}}. \tag{A.6}$$

It is easily established that the lower bound χ_{mf}, considered as a function of the decoupling parameter ρ, is optimized when

$$\rho = \bar{n}. \tag{A.7}$$

From (A.5), (A.6) and (A.7) the optimal *fugacity-driven* mean-field lower bound for χ is

$$\chi \geq \chi_{VW} \tag{A.8}$$

$$\equiv \max_{\rho} \chi_{mf} \tag{A.9}$$

$$= \log(1 + 2z\, e^{2\beta\rho} + z^2\, e^{4\beta\rho}\, e^{-\beta U}) - \beta\rho^2 \tag{A.10}$$

where ρ is the solution of

$$\rho = \frac{2z\, e^{2\beta\rho}(1 + z\, e^{2\beta\rho}\, e^{-\beta U})}{1 + 2z\, e^{2\beta\rho} + z^2\, e^{4\beta\rho}\, e^{-\beta U}} \tag{A.11}$$

which maximizes (A.10).

We next determine an upper bound for χ by means of the functional integral method. We consider the J_{ij} to be entries of a matrix J. From (1.3) J_{ij} is real symmetric. We further assume that J is positive definite. Applying the standard functional integral representation [11]

$$\exp\left[\beta \sum_{ij} J_{ij} n_i n_j\right] = \left(\frac{\beta}{\pi}\right)^{V/2} (\mathrm{Det}\, J)^{-1/2} + \int_{\mathbb{R}^V} \mathfrak{D}x \exp\left[-\beta \sum_{ij} J_{ij}^{-1} x_i x_j\right] \exp\left[2\beta \sum_i x_i n_i\right] \tag{A.12}$$

$$\mathfrak{D}x \equiv \prod_i \mathrm{d}x_i \tag{A.13}$$

with (1.2) and (2.1) we obtain

$$\mathcal{Q} = (\beta/\pi)^{V/2} (\mathrm{Det}\, J)^{1/2} \int_{\mathbb{R}^V} \mathfrak{D}x \exp\left[-\beta \sum_{ij} J_{ij}^{-1} x_i x_j\right] \mathrm{Tr} \exp\left[\beta \left(\sum_i [n_{i\uparrow} n_{i\downarrow} + (2x_i - \mu) n_i]\right)\right]. \tag{A.14}$$

Computing the trace and adding and subtracting a diagonal term to the exponent in (A.14) we arrive at

$$Q = (\beta/\pi)^{V/2} (\mathrm{Det}\, J)^{-1/2} \int_{\mathbb{R}^V} \mathfrak{D}x \exp\left[-\beta \sum_{ij} (J_{ij}^{-1} - (1-\varepsilon)^{-1}\delta_{ij}) x_i x_j\right] e^{V\chi\{x\}} \tag{A.15}$$

where $0 < \varepsilon < 1$

$$\chi\{x\} \equiv \frac{1}{V} \sum_i \log(1 + 2z\, e^{2\beta x_i} + z^2\, e^{4\beta x_i} + z^2\, e^{4\beta x_i}\, e^{-\beta U}) - \frac{\beta}{V(1-\varepsilon)} \sum_i x_i^2 \tag{A.16}$$

and we have made use of (1.4).

It then follows that

$$\mathcal{Q} \leqslant e^{V\chi_{\max}}\, \mathrm{Det}(I - J/(1-\varepsilon)) \tag{A.17}$$

where

$$\chi_{\max} \equiv \max_{x \in \mathbb{R}^V} \chi\{x\} \tag{A.18}$$

and we have used (A.12) assuming that the matrix $J-I/(1-\varepsilon)$ is positive definite. This is indeed the case because from (1.3) J is cyclic and has eigenvalues

$$\lambda_k=\sum_j J(\|j\|)\,e^{2\pi ij.k/L} \tag{A.19}$$

and hence (from (1.4)) the maximum eigenvalue of J is 1.

Elementary differentiation establishes that

$$\chi_{\max}=\chi_{vw}+O(\varepsilon) \tag{A.20}$$

the subdominant term being independent of V. From (2.2), (A.17) and (A.20) then

$$\chi\leqslant\chi_{vw}+V^{-1}\log\mathrm{Det}(I-J/(1-\varepsilon))+O(\varepsilon)+O(V^{-1}). \tag{A.21}$$

Now it has been shown [12] that

$$\lim_{V\to\infty} V^{-1}\log\mathrm{Det}(I-J/(1-\varepsilon))$$

vanishes in the infinite-dimensional limit ($d\to\infty$) and also in the Kac limit ($\gamma\to 0^+$) if $\tilde{J}(x)$ is of the form

$$\tilde{J}(x)=\gamma^d K(\gamma x) \tag{A.22}$$

where K is a positive, integrable and monotone decreasing function.

It follows from (A.8) and (A.21) that χ and χ_{vw} equate in the $d=\infty$ and Kac limits. It is a simple exercise to check that ψ_{vw} is the Helmholtz free energy corresponding to χ_{vw} and hence that ψ and ψ_{vw} equate in the $d=\infty$ and Kac limits.

References

[1] Micnas R, Ranninger J, Robaszkiewicz S and Tabor S 1988 *Phys. Rev.* B **37** 9410
[2] Micnas R, Ranninger J and Robaszkiewicz S 1989 *Phys. Rev.* B **39** 11 653
[3] Micnas R, Ranninger J and Robaszkiewicz S 1990 *Rev. Mod. Phys.* **62** 113
[4] Thompson C J 1992 *Prog. Theor. Phys.* **87** 535
[5] Janis V and Vollhardt D 1992 *Int. J. Mod. Phys.* B (Singapore) **6** 731
[6] Van Dongen P G J and Vollhardt D 1990 *Phys. Rev. Lett.* **65** 1663
[7] Bursill R J and Thompson C J 1993 *Variational bounds for lattice fermion models I Spinless fermions* To appear in *J. Phys. A*
[8] Matsubara T Private communication
[9] Thompson C J 1988 *Classical Equilibrium Statistical Mechanics* (Oxford: Oxford University Press)
[10] Whangbo M H and Toradi C C 1990 *Science* **249** 1143
[11] Cramer H 1951 *Mathematical Methods in Statistics* (Princeton: Princeton University Press)
[12] Cant A and Pearce P A 1983 *Commun. Math. Phys.* **90** 373